ORIGINAL ARTICLE

INTERNATIONAL JOURNAL OF RESEARCH IN PHARMACEUTICAL SCIENCES

Published by JK Welfare & Pharmascope Foundation Journal Home Page: https://ijrps.com

Synthesis and characterization of new imidazole azo ligand with some of transition metal ions, and their biological effect on two pathogenic bacteria of burn patients

Israa N. Witwit[1], Husham M. Mubark[1], Hutham Mahmood Yousif Al-Labban[1], Ahmed abduljabbar jaloob aljanaby[*2]

[1]Department of Chemistry, University of Kufa, Factualy of Science, Najaf, Iraq
[2]Department of Biology, University of Kufa, Faculty of Science, Iraq

Article History:

Received on: 15.03.2019
Revised on: 20.06.2019
Accepted on: 24.06.2019

Keywords:

imidazole azo,
metal complexes,
burn patients,
biological activity,
Staphylococcus aureus,
Pseudomonas aeruginosa

ABSTRACT

New imidazole azo ligand (DPIDA) was prepared by coupling reaction between 4,5-di phenyl imidazole and N1,N1-dimethylbenzene1,4-diamine di hydrochloride and studied the complexation of this ligand with Mn(II) , Co(II) , Ni(II) , Cu(II) , Zn(II) , Cd(II) , and Hg(II) ions , The free ligand and it's complexes characterized by Mass, ^{1}HNMR, IR, UV-Vis. , and molar conductivity that indicated the octahedral geometry of them with a bidentate ligand which coordinated from (N3) atom of imidazole ring and one nitrogen atom of azo group.Biological activity of ligand (DPIDA) and it's complexes tested against two multi-drug resistant aerobic pathogenic bacteria isolated from patients with a burn. Three concentrations were selected (50, 100, 150) mg/ml for each crud synthesized derivative compounds. The derivative compound (4,5-diphenyl imidazole) with concentration 150mg/ml had an excellent antibacterial effect against *Staphylococcus aureus* and *Pseudomonas aeruginosa* with inhibition zone 21.83 $\pm$ 0.1764 mm and 24.30 $\pm$ 0.4163 mm respectively.

*Corresponding Author

Name: Ahmed abduljabbar jaloob aljanaby
Phone:
Email: ahmedaj.aljanabi@uokufa.edu.iq

ISSN: 0975-7538

DOI: https://doi.org/10.26452/ijrps.v10i3.1382

Production and Hosted by

IJRPS | https://ijrps.com

INTRODUCTION

Heterocyclic azo compounds have a lot of scientific attention especially in the last five decades because of their applications in different of applied and academic fields such as Analytical reagents (Cheira *et al.*, 2012), antibacterial (Witwit *et al.*, 2018), antifungal (Slassi *et al.*, 2019a) anticancer (Vernieuwe *et al.*, 2017) and Optical electrical switching of liquid crystals (Oh *et al.*, 2017). Imidazole azo ligands considered as an essential type of heterocyclic azo ligands chiefly in coordination chemistry due to their ability to form stable complexes with metal ions in various of oxidation states (Al-Adilee and Kyhoiesh, 2017), formation of stable five-member ring with each ion through (N3) atom of imidazole ring and one of nitrogen atoms of azo group (Al-Muhanaa and Al-Khafagy, 2018). As well as the contribution of imidazole molecule in preparation of many ligands which have π – conjugated system that increases their stability and follows the colour change of them before and after the coordination with metal ions (Erbaş and Gülle, 2018). The goal of this research is representing by preparation and characterization of new ligand as a derivative of 4,5-diphenylimidazole, studying it's coordination behavior with Mn(II) , Co(II) , Ni(II) , Cu(II) , Zn(II) , Cd(II) , and Hg(II), and experienced their biological activity against two types of multi-drug resistant aerobic pathogenic bacteria have isolated from burn patients.

MATERIALS AND METHODS

Chemicals and Instruments

All chemicals and solvents were equipped with high purity from Sigma Aldrich, BDH and Merck companies. Mass Spectrum was measured using AB SCIEX 3200 QTRAP Mass analyzer , FT-IR carried out by Shimadzu FTIR8400 using KBr disks from (400-4000)cm^{-1} Electronic spectrum measured by Shimadzu UV-1650 UV-Vis Spectrophotometer , The element analysis performed on Costech ECS Elemental 4010, magnetic measurements of prepared complexes recorded by Balance Magnetic Susceptibility Model –M.S.B Auto , Molar conductivity menstruated via 720(WTW), and ^{1}HNMR carried out by Bruker Avance-111 300 MHz NMR Spectrometer.

Preparation of (DPIDA) ligand

Two and thirty-one gram of N1, N1-dimethylbenzene1,4-diamine dihydrochloride was dissolved in twenty-five ml of distilled water than one ml of hydrochloric acid added gradually to this solution which cooled in ice bath 0-5 ^{o}C, the formation of diazonium salt occurred by addition the solution of sodium nitrate which prepared by dissolved 0.70 gm of it in 10 ml of distilled water drop by drop with stirring, This solution leaved in the ice bath for 30 minute then coupled with alcoholic solution of 4,5- diphenyl imidazole which prepared by dissolving 2.21 gm of imidazole derivative and 0.44 gm of sodium hydroxide in 25 ml of ethanol, orange precipitate was appeared after the completing of addition, filtered and dried then recrestalysid from ethanol yield percentage 71 % as shown in Scheme 1.

Preparation of complexes (general method)

All complexes were prepared with mole ratio 1:2 (metal: ligand) by mixing 1 mmole of metal chlorides in twenty-five ml of distilled water with 2 m moles of (DPIDA) in twenty-five ml of ethanol with stirring until the precipitations of the complexes were appeared, filtered and dried the yield percentage of them were shown in Table 1.

Biological Activity

Biological activity testing was done to detect the antibacterial activity of four synthesized derivatives compounds against two multi-drug resistant aerobic pathogenic bacteria isolated from patients with burn infection; Staphylococcus aureus (*S.aureus*) is a gram-positive bacteria and pseudomonas aeruginosa (*P.aeruginosa*) as a gram harmful bacteria. The two pathogenic bacteria were provided with kindly from the university of Kufa, Faculty of science, department of microbiology, Iraq. Antibacterial activity test was done according to the agar well diffusion method (Aljanaby, 2013, 2018). Three concentrations were selected (50, 100, 150) mg/ml for each crud synthesized derivative compounds. Four wells were made by crock-poorer (Oxoid, UK) in Muller-Hinton agar surface (Oxoid, UK) and swabbed with two pathogenic bacteria with turbidity according to 0.5 McFarland tube. Fifty μl of each dilution was transferred to each well and left at (20)^{o}C for 3 hours and incubated at (37)^{o}C for 24 hours. Four replicates were done for each test. The inhibition zone around each well was measured in millimetres (Adam *et al.*, 2019; Aljanaby and Alhasnawi, 2017).

Statically analysis

Graph pad prism V.6 windows soft were been used in statically analysis to compare between diameters of inhibition zone (mm) according to T-test. P-value < 0.05 was considered indicative of statistically significant (Adam *et al.*, 2019).

RESULTS AND DISCUSSION

^{1}HNMR spectra of free ligand (DPIDA) in (d^{6} DMSO) inhibit a singlet signal in (3.03) ppm due to the protons of (N-CH_3) groups, whilst the siglet signal of (N-H) for imidazole ring (Rehab *et al.*, 2016) appeared in (12.63) ppm, this spectrum confirms the number of protons in the molecular structure, as shown in Figure 1.

Mass spectrum of (DPIDA) ligand showed molecular ion peak(M+1) at m/e (368) , the initial fragmentation started by losing (-N_2) molecule at m/e (340) , while the base peak appeared at (e/z= 221) corresponding to 4,5- diphenylimidazole fragment ($C_{15}H_{12}N_2$) (Mehdi and Ali, 2005). The spectrum of $Mn(DPIDA)_2Cl_2$ complex exhibited molecular peak at (e/z = 860) that affirmed the molecular weight of this complex, the fragmentation also started by losing the nitrogen's of the two coordinated azo ligands at (e/z=804) and continued to the last step which showed the fragment of 4,5- diphenylimidazole as base peak, theFigures 2 and 3 and Schemes 2 and 3 illustrated the fragmentation of ligand, and it's complicated.

Uv-Vis spectrum of free ligand (DPIDA) show up three bands at 284, 257, 238 nm which attributed to ($\pi - \pi^*$) transitions of aromatic rings which shifted to higher wavelengths with little changes of values in complexes spectrums , while the bands at 466 nm of (n-π^*) transitions that exhibited redshift in the ranges of complexes as a result of charge transfer transitions after coordination as shown in Table 2.

IR spectra of ligand (DPIDA) showed v(N-H) peak

Table 1: Some of the physicochemical properties of (DPIDA) ligand and it's complexes

Compound (Empirical Formula)	Mwt	Yield (%)	Elemental Analysis Calcl. (Found)				m.p (oC)
		C%	H%	N%	M%		
(DPIDA) ($C_{23}H_{21}N_5$)	367.46	71	75.18 (75.20)	5.76 (5.73)	19.06 (19.08)	——	232-234
[Mn(DPIDA)$_2$Cl$_2$] ($C_{46}H_{42}Cl_2N_{10}Mn$)	860.75	68	64.19 (64.22)	4.92 (4.94)	16.27 (16.25)	6.38 (6.40)	310-312
[Co(DPIDA)$_2$Cl$_2$] ($C_{46}H_{42}Cl_2N_{10}Co$)	864.75	75	63.89 (63.00)	4.90 (4.90)	16.20 (16.23)	6.82 (6.79)	325-328
[Ni(DPIDA)$_2$Cl2] ($C_{46}H_{42}Cl_2N_{10}Ni$)	864.51	78	63.91 (63.95)	4.90 (4.92)	16.20 (16.20)	6.79 (6.82)	332-334
[Cu(DPIDA)$_2$Cl$_2$] ($C_{46}H_{42}Cl_2N_{10}Cu$)	869.36	72	63.55 (63.52)	4.87 (4.90)	16.11 (16.12)	7.31 (7.34)	346-348
[Zn(DPIDA)$_2$Cl$_2$] ($C_{46}H_{42}Cl_2N_{10}Zn$)	871.19	74	63.42 (63.42)	4.86 (4.88)	16.08 (16.05)	7.50 (7.52)	353-355
[Cd(DPIDA)$_2$Cl$_2$] ($C_{46}H_{42}Cl_2N_{10}Cd$)	918.22	71	60.17 (60.18)	4.61 (4.60)	15.25 (15.26)	12.24 (12.30)	364-367
[Hg(DPIDA)$_2$Cl$_2$] ($C_{46}H_{42}Cl_2N_{10}Hg$)	1006.40	84	54.90 (54.93)	4.21 (4.19)	13.92 (14.00)	19.93 (19.88)	375-377

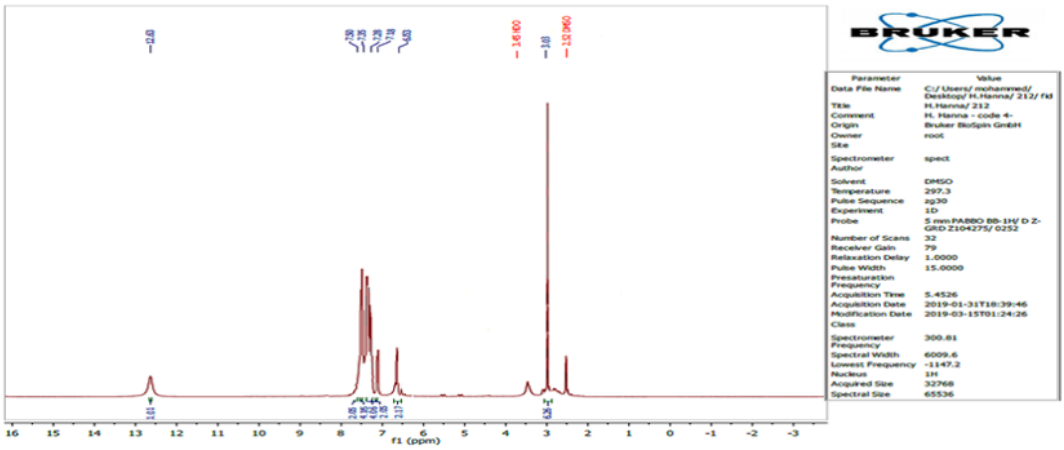

Figure 1: ^{1}HNMR spectrum of (DPIDA) ligand in d^{6}DMSOsolvent

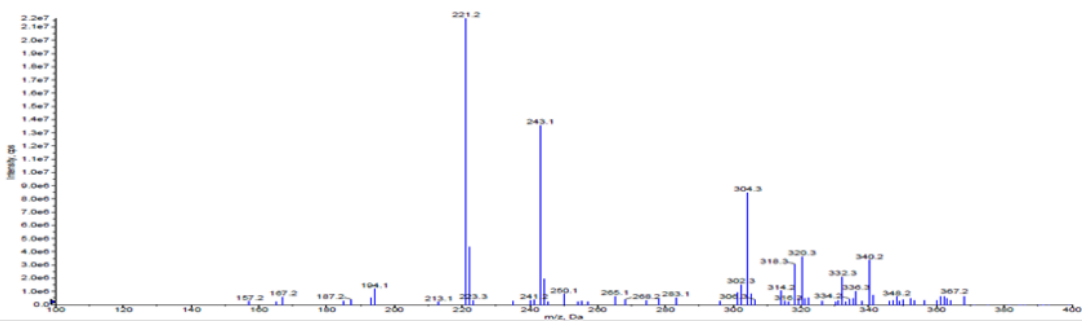

Figure 2: Mass spectrum of (DPIDA) ligan

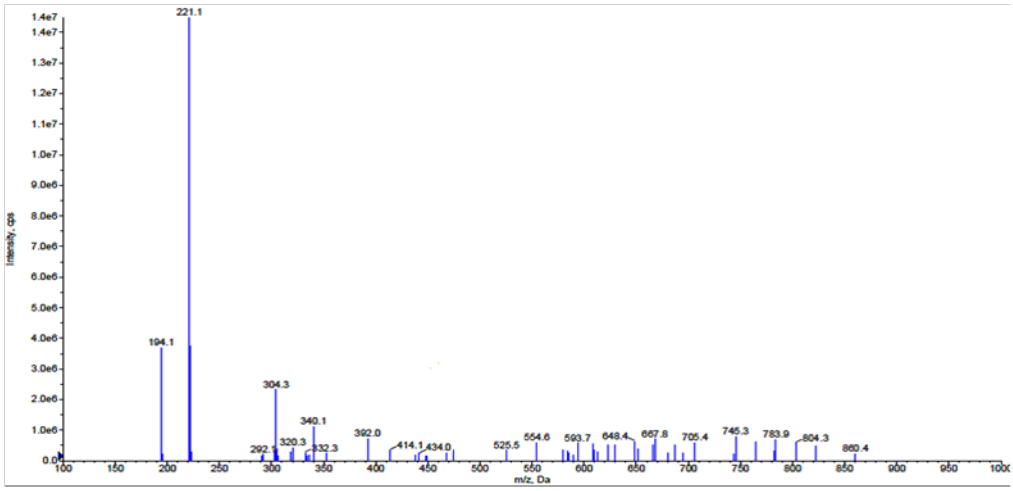

Figure 3: Mass spectrum of Mn (II) complex

Table 2: Molar Conductivity, Magnetic Susbtibility and Electronic Transitions of ligands and their complexes

Compound	Molar Conductivity S.Cm^2.mole		μ.eff. (B.M.)	λ max (nm)	Transitions	Geometry
	DMF	DMSO				
(DPIDA)	—–	——-	—–	284, 257, 238 466	π-π* C.T	—–
[Mn(DPIDA)$_2$Cl$_2$]	23.6	20.6	5.74	281,242, 304 472	π-π* MLCT	Octahedral
[Co(DPIDA)$_2$Cl$_2$]	21.8	18.3	4.70	280, 250, 230 536	π-π* MLCT	Octahedral
[Ni(DPIDA)$_2$Cl$_2$]	21.7	18.2	2.84	281, 254 , 230 550	π-π* MLCT	Octahedral
[Cu(DPIDA)$_2$Cl$_2$]	20.5	17.1	1.73	278, 254, 232 536	π-π* MLCT	Distorted Octahedral
[Zn(DPIDA)$_2$Cl$_2$]	18.3	14.6	Dia	274,250,232 485	π-π* MLCT	Octahedral
[Cd(DPIDA)$_2$Cl$_2$]	17.8	13.2	Dia	244, 276 , 308 468	π-π* MLCT	Octahedral
[Hg(DPIDA)$_2$Cl$_2$]	15.4	11.7	Dia	286 , 254, 230 504	π-π* MLCT	Octahedral

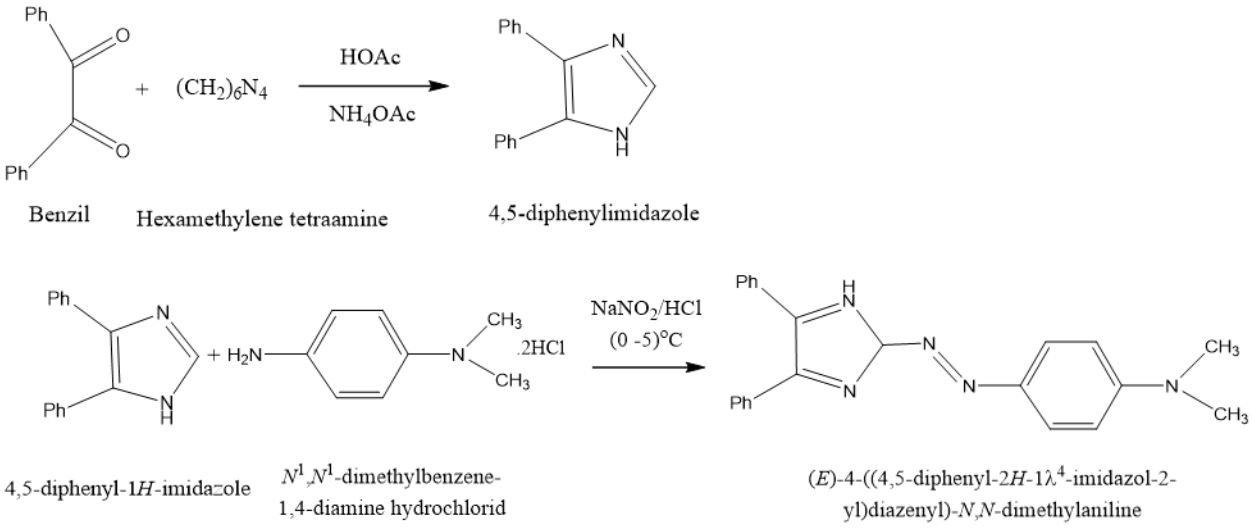

Scheme 1: Preparation of (DPIDA) ligand

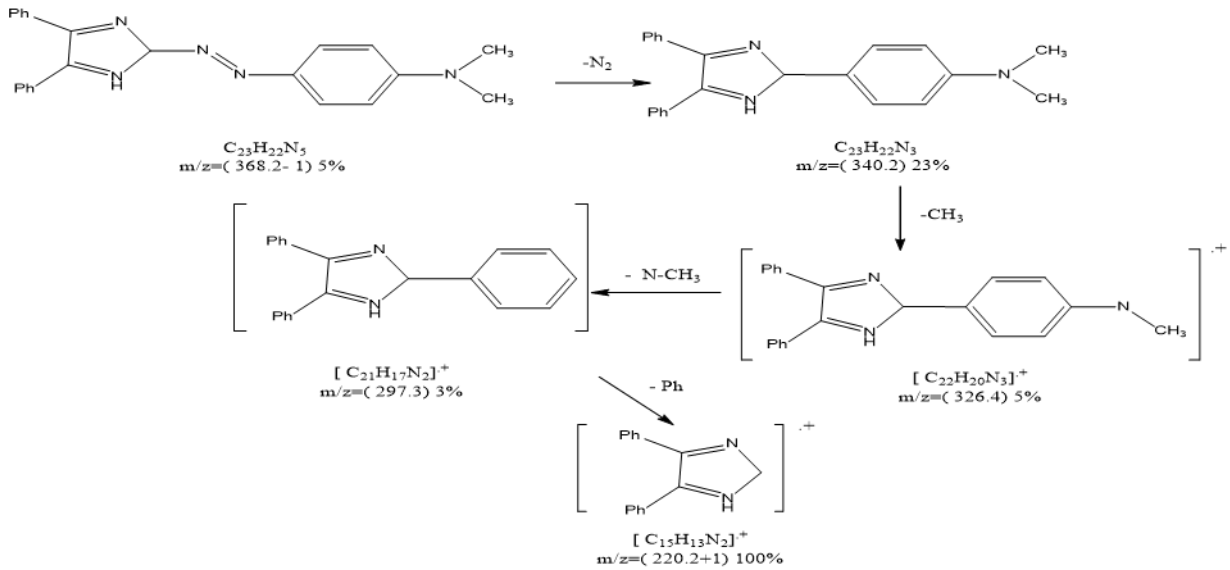

Scheme 2: Mass Fragmentation of (DPIDA) ligand

Table 3: IR frequencies of ligand and it's complexed

Compound	v(N-H) imidazole	v (C=N) imidazole	v(N=N)	v(C-N) imidazole	v(M-N)
(DPIDA)	3400 w	1588 m	1498 m	1315 m	-
$[Mn(DPIDA)_2Cl_2]$	3403 w	1572 m	1489m	1325 m	543 w
$[Co(DPIDA)_2Cl_2]$	3400 w	1570 m	1486 m	1328 m	540 w
$[Ni(DPIDA)_2Cl_2]$	3405 w	1566 m	1484 m	1320 m	435 w
$[Cu(DPIDA)_2Cl_2]$	3400 w	1575 m	1489 m	1323 m	511 w
$[Zn(DPIDA)_2Cl_2]$	3402 w	1568 m	1488 m	1321 m	525 w
$[Cd(DPIDA)_2Cl_2]$	3402 w	1570 m	1482 m	1324 m	532 w
$[Hg(DPIDA)_2Cl_2]$	3400 w	1565 m	1485 m	1324 m	523 w

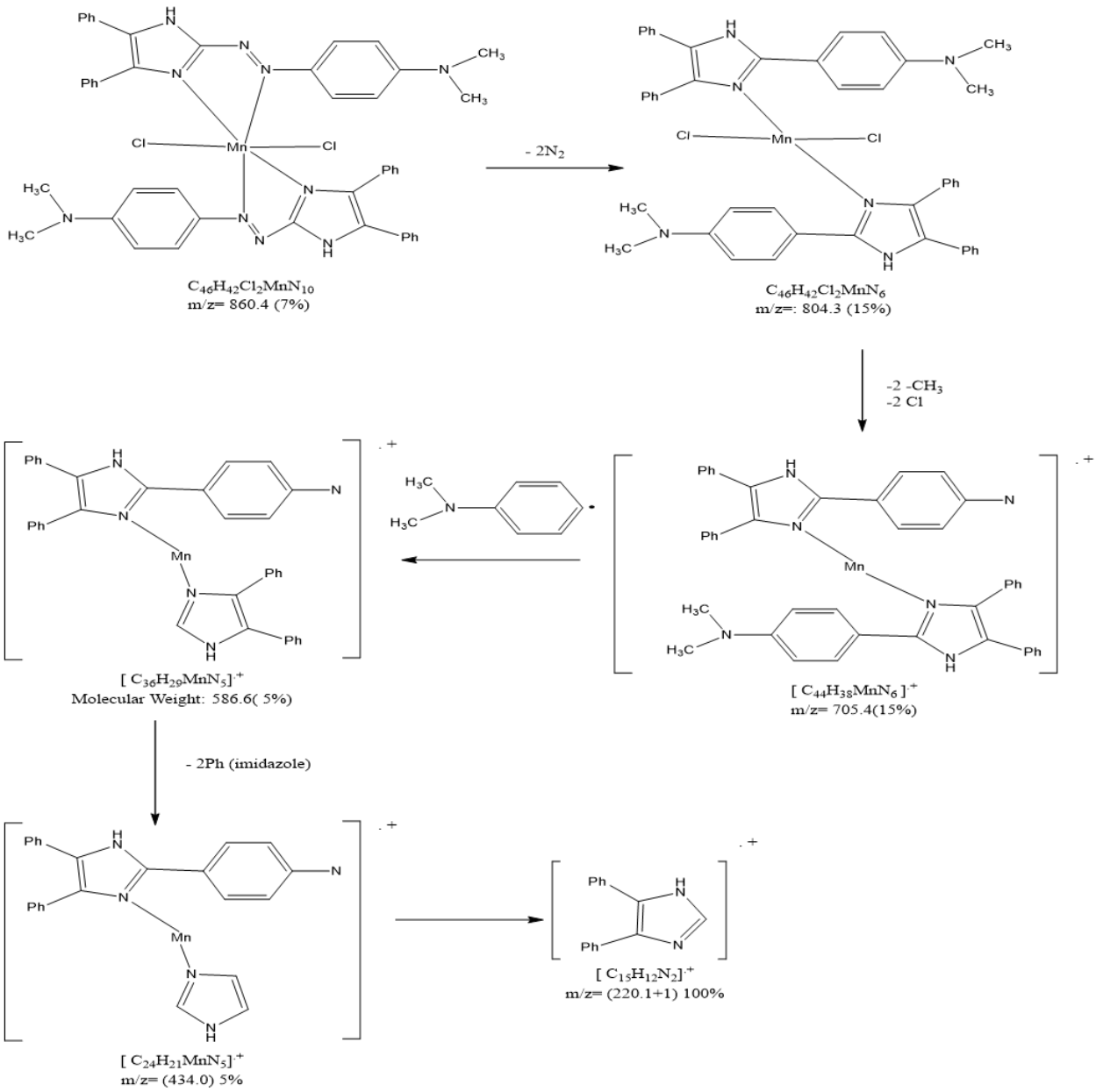

Scheme 3: Mass Fragmentation of Mn (II) Complex

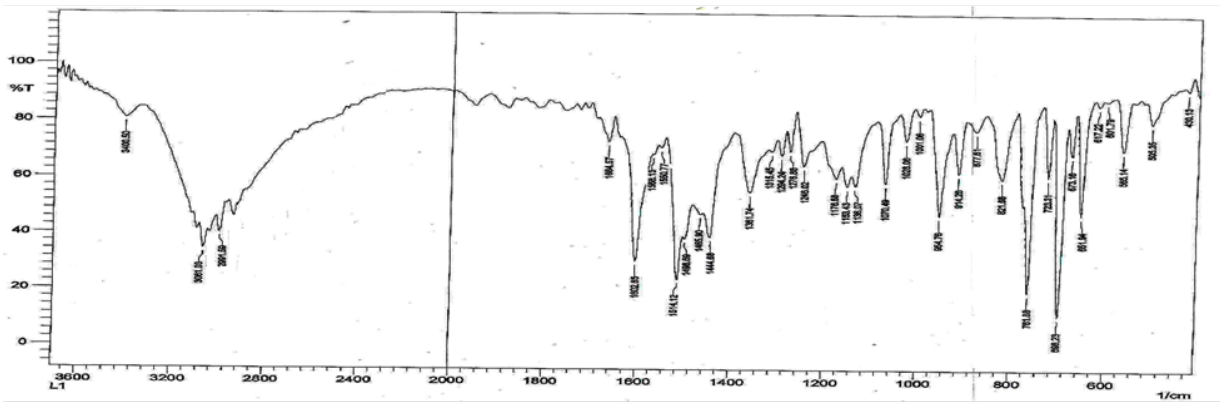

Figure 4: IR spectrum of (DPIDA) ligand

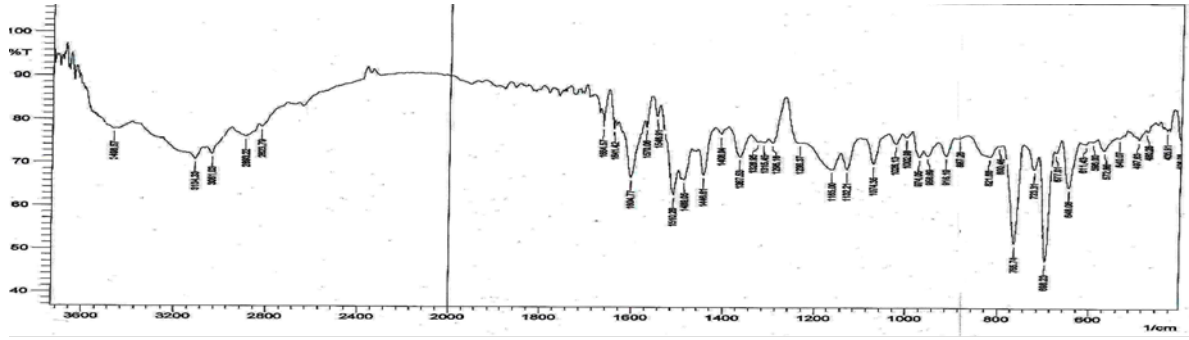

Figure 5: IR spectrum of Co (II) complex

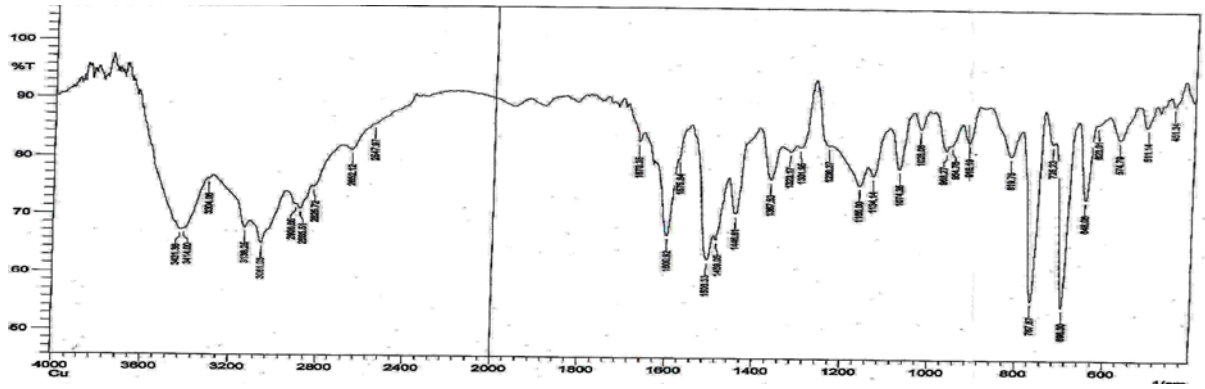

Figure 6: IR spectrum of Cu (II) complex

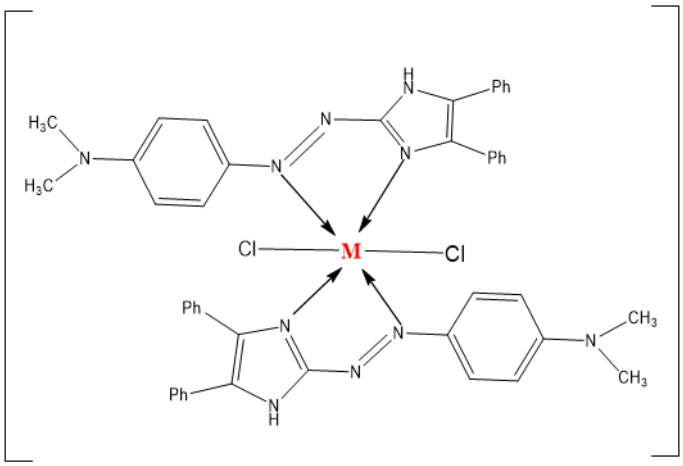

Figure 7: Suggested structure of [M(DPIDA)$_2$ Cl$_2$]

of imidazole ring at (3400) cm$^-$ (Abbas and Kadhim, 2016) two peeks at (3034) and (3061) cm- due to the vibrations of aromatic v(C-H) , and one peak at (2991) cm- of aliphatic v(C-H) that showed no significant changes in the spectra of the complexes frequencies. The peaks at (1588) cm- and (1315) cm- exhibited a stretching of v(C=N) and v(C-N) (Al-Hasani and Almaliky, 2015) respectively of imidazole ring that proceed a changing in position and intensity in complexes which is an indicate the participation of (N3) atom in coordination, also the values of v(N=N) (Jarad and Kadhim, 2018; Slassi *et al.*, 2019b) peak at (1498) cm- shifted to lower values in the complexes that's considered as an evidence on coordination proceed through one nitrogen atom of azo group, new values of v(M-N) frequencies appeared between (543 -511) cm$^-$ in the complexes that consider as additional evidence on coordination process as shown in Table 3 and Figures 4, 5 and 6.

Conductivity measurements at 25°C in both of DMF and DMSO solvents for (10^{-3}) M encouraged non- ionic character of all complexes , The values of molar conductivity ranged between 23.6-15.4

Table 4: Antibacterial activity of four derivative compounds against two types of aerobic pathogenic bacteria isolated from patients with burns infections

Derivative compounc	Multi-drug resistance aerobic pathogenic bacteria			
	S.aureus		P.aeruginosa	
	Concentration	ME± SE, R=4	Concentration	ME± SE, R=4
(DPIDA)	50 mg/ml	5.4667 ± 0.42557	50 mg/ml	4.8667 ± 0.43333
	100 mg/ml	7.7667 ± 0.29627	100 mg/ml	7.6333 ± 0.088192
	150 mg/ml	8.7333 ± 0.12019	150 mg/ml	8.9000 ± 0.11547
Hg complex	50 mg/ml	9.4333 ± 0.23333	50 mg/ml	9.7333 ± 0.088192
	100 mg/ml	9.6667 ± 0.12018	100 mg/ml	10.033 ± 0.12019
	150 mg/ml	10.367 ± 0.12019	150 mg/ml	10.833 ± 0.14530
Zn Complex	50 mg/ml	11.500 ± 0.20817	50 mg/ml	11.960 ± 0.070238
	100 mg/ml	12.037 ± 0.051747	100 mg/ml	12.617 ± 0.29946
	150 mg/ml	12.033 ± 0.10899	150 mg/ml	12.593 ± 0.19548
Cu Complex	50 mg/ml	12.17 ± 0.1901	50 mg/ml	12.95 ± 0.02333 N
	100 mg/ml	12.42 ± 0.1654	100 mg/ml	12.43 ± 0.2010
	150 mg/ml	12.72 ± 0.1352	150 mg/ml	12.72 ± 0.1251
Co Complex	50 mg/ml	11.767 ± 0.24037	50 mg/ml	12.567 ± 0.20276
	100 mg/ml	12.000 ± 0.26458	100 mg/ml	12.833 ± 0.033333
	150 mg/ml	14.900 ± 0.40415	150 mg/ml	15.733 ± 0.088192
Mn Complex	50 mg/ml	14.830.09536=3	50 mg/ml	14.72 ± 0.1844
	100 mg/ml	15.28 ± 0.1802	100 mg/ml	16.07 ± 0.07142
	150 mg/ml	16.11 ± 0.1068	150 mg/ml	16.74 ± 0.1949
Cd Complex	50 mg/ml	18.61 ± 0.2275	50 mg/ml	18.52 ± 0.2217
	100 mg/ml	18.81 ± 0.1757	100 mg/ml	18.70 ± 0.1695
	150 mg/ml	18.86 ± 0.2781	150 mg/ml	19.51 ± 0.2623
4,5-diphenyl imidazol	50 mg/ml	17.833 ± 0.17638	50 mg/ml	18.700 ± 0.11547
	100 mg/ml	18.767 ± 0.17638	100 mg/ml	19.533 ± 0.17638
	150 mg/ml	21.83 ± 0.1764	150 mg/ml	24.30 ± 0.4163

C: Concentrationsof derivative compounds, R: Numbers of replicates, M: Mean of the diameter ofinhibition zone (mm), SE: Standard error of the mean

S.cm^2.mole in DMF , while their values within 20.6-11.7 S.cm^2.mole, as well no white precipitate of AgCl observed when a drops of 0.1 N from $AgNO_3$ solution to metal complexes solutions added which also confirms the absence of counter ion outside the coordination sphere (Reddy *et al.*, 1997; Hayder and Aljanaby, 2019) as apparent in Table 2. The suggested structure of the complexes showed the octrahyral geometry that two (DPIDA) ligands coordinated with central metal ion as bidentate through nitrogen atom number 3 of imidazole ring and one nitrogen atom of the azo group as explained in Figure 7.

The results of biological activity demonstrated that most the ligand and complexes have good antibacterial activity against two pathogenic bacteria with inhibition zones in three concentrations Table 4 andFigure 8 and Figure 9 While, the derivative compound 4,5-diphenyl imidazol with concentration 150mg/ml had excellent antibacterial effect against S.aureus and P.aeruginosa with inhibition zone 21.83 ± 0.1764 mm and 24.30 ± 0.4163 mm respectively.

CONCLUSION

Seven complexes of Mn(II) , Co(II) , Ni(II) , Cu(II) , Zn(II) , Cd(II) , and Hg(II) ions with new imidazole azo ligand (DPIDA) were prepared as an octahedral geometry of them with bidentate ligand with general formal [M $(DPIDA)_2Cl_2$] the prepared compounds showed excellent biological activity against two types of bacteria *S.aureus and P.aeruginosa*.

REFERENCES

Abbas, A., Kadhim, R. S. 2016. Preparation, Spectral and Biological Studies of Azo Ligand Derived from Proline with Cu(II), Ag(I) and Au(III) Metal

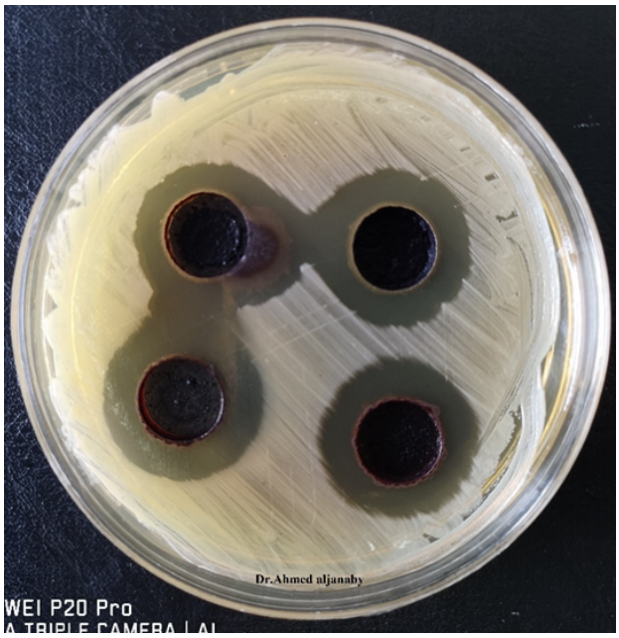

Figure 8: Antibacterial activity test of the 4,5-diphenyl imidazol derivative compound with concentration 150gm/ml against multi-drug resistance S.aureus isolated from patients with burns infections

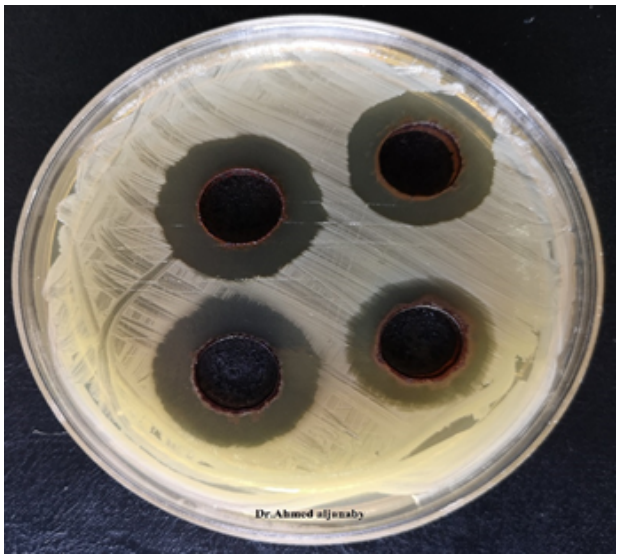

Figure 9: Antibacterial activity test of the 4,5-diphenyl imidazol derivative compound with concentration 150 gm/ml against multi-drug resistance P.aeruginosa isolated from patients with burns infections

Ion. *IOSR Journal of Applied Chemistry*, 9(8):20–31.

Adam, R. W., Al-Labban, H. M. Y., Aljanaby, A. A. J., Abbas, N. A. 2019. Synthesis, Characterization and Antibacterial Activity of Some New of. *Novel*, 1(2):99–110.

Al-Adilee, K., Kyhoiesh, H. A. 2017. Preparation and identification of some metal complexes with new heterocyclic azo dye ligand 2-[2—-(1-Hydroxy-4-Chloro phenyl) azo]-imidazole and their spectral and thermal studies. *Journal of Molecular Structure*, 1137:160–178.

Al-Hasani, T. J., Almaliky, Z. S. 2015. New Pd and Pt Complexes of Guanine–Azo Dye: Structural, Spectroscopic, Dyeing Performance and Antibacterial Activity Studies. *Iraqi Journal of Science*, 56(4):2718–2731.

Al-Muhanaa, S. S., Al-Khafagy, A. H. 2018. Preparation and Biological Activities of New Heterocyclic Azo Ligand and Some of Its Chelate Complexes. *Nano Biomedicine and Engineering*, 10(1):10–5101.

Aljanaby, A. A. J. 2018. Antibacterial activity of an aqueous extracts of Alkanna tinctoria roots against drug resistant aerobic pathogenic bacteria isolated from patients with burns infections. *Russian Open Medical Journal*, 7(1):0104.

Aljanaby, A. A. J., Alhasnawi, H. M. R. J. 2017. Phenotypic and molecular characterization of multidrug resistant Klebsiella pneumoniae isolated from different clinical sources in Al-Najaf Province-Iraq. *Pakistan Journal of Biological Sciences*, 20(5):217–232.

Aljanaby, A. A. J. J. 2013. Antibacterial activity of an aqueous extract of Petroselinum crispum leaves against pathogenic bacteria isolated from patients with burns infections in Al-najaf Governorate Iraq. *Research on Chemical Intermediates*, 39(8):3709–3714.

Cheira, M. F., Khawassek, Y., Hussein, G. 2012. Studies on the extraction of copper (II) by pyrazoloquinazolinone derivatives from aqueous solutions. *Research Journal of Chemical Sciences*, 2(6):30–37.

Erbaş, S. Ç., Gülle, S. 2018. Synthesis and Photophysical Behaviours of Novel Phenanthro [9, 10-d] imidazole Substituted Azo Dyes in Solvent Media. *Celal Bayar Üniversitesi Fen Bilimleri Dergisi*, 14(3):285–289.

Hayder, T., Aljanaby, A. A. J. J. 2019. Antibiotics susceptibility patterns of Citrobacter freundii isolated from pa-tients with urinary tract infection in Al-Najaf governorate–Iraq. *International Journal of Research in Pharmaceutical Sciences*, 10(2):1481–1488.

Jarad, Kadhim, S. 2018. Synthesis, Spectral Studies and Biological Activity of Azo dye Complexes with Some MetalIons. *Journal of Global Pharma Technology*, 10(06):97–106.

Mehdi, R. T., Ali, A. M. 2005. Preparation and characterization of new azo imidazole ligand and some Transition Metal Complexes. *Iraqi National Journal of Chemistry*, 20:540–546.

Oh, S. W., Baek, J. M., Kim, S. H., Yoon, T. H. 2017. Optical and electrical switching of cholesteric liquid crystals containing azo dye. *RSC Advances*, 7(32):19497–19501.

Reddy, K. H., Reddy, M. R., Raju, K. M. 1997. Synthesis, characterization, electrochemistry and axial ligation properties of macrocyclic divalent metal complexes of acetylacetone buckled with different diamines. *Polyhedron*, 16(15):2673–2679.

Rehab, Al-Hassani, Journal, B. S. 2016. Synthesis, Characterization, Antimicrobial and Theoretical Studies of V(IV),Fe(III),Co(II),Ni(II), Cu(II), and Zn(II)Complexes with Bidentate (NN) Donar Azo Dye Ligand. *Baghdad Science Journal*, 13(4):793–805.

Slassi, S., Fix-Tailler, A., Larcher, G., Amine, A., El-Ghayoury, A. 2019a. Imidazole and Azo-Based Schiff Bases Ligands as Highly Active Antifungal and Antioxidant Components. *Heteroatom Chemistry*, pages 1–9.

Slassi, S., Fix-Tailler, A., Larcher, G., Amine, A., El-Ghayoury, A. 2019b. *Imidazole and Azo-Based Schiff Bases Ligands as Highly Active Antifungal and Antioxidant Components*. Heteroatom Chemistry.

Vernieuwe, K., Cuypers, D., Kirschhock, C. E. A., Houthoofd, K., Vrielinck, H., Lauwaert, J., Buysser, K. D. 2017. Thermal processing of aqueous AZO inks towards functional TCO thin films. *Journal of Alloys and Compounds*, 690:360–368.

Witwit, I. N., Motaweq, Z. Y., Mubark, H. M. 2018. Synthesis, characterization, and biological efficacy on new mixed ligand complexes based from azo dye of 8-hydroxy quinoline as a primary ligand and imidazole as a secondary ligand with some of transition metal ions. *Journal of Pharmaceutical Sciences and Research*, 10(12):3074–3083.

